MAPS: Multi-Fidelity AI-Augmented Photonic Simulation and Inverse Design Infrastructure

Pingchuan Ma[1], Zhengqi Gao[2], Meng Zhang[3], Haoyu Yang[4], Mark Ren[4],
Rena Huang[3], Duane S. Boning[2], Jiaqi Gu[1†]
[1]Arizona State University, [2]Massachusetts Institute of Technology, [3]Rensselaer Polytechnic Institute, [4]NVIDIA
†jiaqigu@asu.edu

Abstract*—Inverse design has emerged as a transformative approach for photonic device optimization, enabling exploration of high-dimensional, non-intuitive design spaces to create ultra-compact, high-performance devices, advancing photonic integrated circuits (PICs) in computing and interconnects. However, practical challenges, such as suboptimal device performance compared to manual designs, limited manufacturability, high sensitivity to variations, computational inefficiency, and lack of interpretability, have hindered its adoption in commercial hardware. Recent advancements in AI-assisted photonic simulation and design offer transformative potential, accelerating simulations and design generation by orders of magnitude over traditional numerical methods. Despite these breakthroughs, the lack of an open-source, standardized infrastructure and evaluation benchmark limits accessibility and cross-disciplinary collaboration. To address this, we introduce `MAPS`, a multi-fidelity AI-augmented photonic simulation and inverse design infrastructure, designed to bridge this gap. `MAPS` features three synergistic components: ❶ `MAPS-Data`: A dataset acquisition framework for generating multi-fidelity, richly labeled device designs using intelligent sampling strategies, providing high-quality data for AI-for-optics research. ❷ `MAPS-Train`: A flexible AI-for-photonics training framework, offering hierarchical data loading pipeline, customizable model construction, support for data- and physics-driven losses, and comprehensive evaluation metrics. ❸ `MAPS-InvDes`: An advanced adjoint method-based inverse design toolkit that abstracts complex physics but exposes flexible optimization steps, integrates pre-trained AI models, and incorporates fabrication-aware variation models, for real-world applicability. This infrastructure `MAPS` provides a unified, open-source platform for developing, benchmarking, and advancing AI-assisted photonic design workflows, accelerating innovation in photonic hardware optimization and scientific machine learning.

I. Introduction

The field of photonics has witnessed significant advancements in recent years, driven by the increasing demands for ultra-compact and high-performance devices in photonic integrated circuits (PICs). These devices are pivotal in addressing the growing needs of modern computing and optical interconnect technologies. Traditional design methodologies, which heavily rely on manual design heuristics and iterative optimization, often fail to fully exploit the complex, high-dimensional design spaces inherent in photonic systems. To overcome these limitations, inverse design has emerged as a powerful paradigm, enabling the systematic exploration of unconventional and non-intuitive device configurations.

Inverse design leverages computational optimization to generate photonic device designs that meet specific performance criteria. By navigating through vast design spaces, this approach has demonstrated remarkable potential in achieving designs that are both compact and highly efficient. However, despite its promise, the practical adoption of inverse design in real-world applications remains constrained by several challenges. These include suboptimal performance compared to manual designs, limited manufacturability due to non-ideal fabrication processes [1]–[3], high sensitivity to variations [4], [5], computational inefficiencies, and the lack of interpretability in design outcomes. Such barriers hinder the transition of inverse-designed devices from research laboratories to commercial hardware.

Recent advancements in artificial intelligence (AI) have opened new avenues for photonic simulation and design. AI-driven methods offer unprecedented acceleration in simulations and optimization processes, achieving speedups that are orders of magnitude faster than traditional numerical techniques [6]–[11]. These advancements have significantly enhanced the feasibility of leveraging inverse design for practical photonic applications. Nonetheless, the broader adoption of AI-assisted approaches in photonics is impeded by the absence of an open-source, standardized infrastructure and evaluation benchmarks. This lack of standardized tools limits accessibility for researchers and prevents effective cross-disciplinary collaboration.

To address these critical gaps, we introduce `MAPS` (Multi-fidelity AI-augmented Photonic Simulation and inverse design), a comprehensive infrastructure that bridges the divide between theoretical advancements and practical implementation. MAPS is designed to be a unified, open-source platform that supports the entire workflow of AI-assisted photonic design. It integrates three core components:

- **`MAPS-Data`:** A dataset acquisition framework that allows flexible sampling strategies to generate multi-fidelity, richly labeled photonic device designs.
- **`MAPS-Train`** A flexible training framework specifically for AI-for-photonics research. This module supports hierarchical data pipelines, customizable model architectures, and physics-driven loss functions while offering comprehensive evaluation metrics.
- **`MAPS-InvDes`** An advanced toolkit for adjoint method-based optimization that abstracts the complexities of photonic physics while incorporating AI models and fabrication-aware variation models for real-world applicability.

978-3-9826741-0-0/DATE25/© 2025 EDAA

II. Preliminary

A. Conventional Photonic Device Inverse Design

The conventional adjoint-method-based photonic device inverse design can be formulated as follows:

$$\begin{aligned} \theta^* &= \underset{\theta\in\Theta}{\operatorname{argmax}}\ F(\epsilon(\theta)|\lambda_c, J), \\ \text{s.t.}\ \ \bar{\rho} &= (\mathcal{G}\circ\mathcal{P})(\theta) \\ \epsilon &= \epsilon_v + (\epsilon_s - \epsilon_v)\cdot\bar{\rho} \\ \mathcal{P}: \theta \in \mathbb{R}^N &\rightarrow \rho \in \{0,1\}^{N^x\times N^y} \\ \mathcal{G}: \rho \in \{0,1\}^{N^x\times N^y} &\rightarrow \bar{\rho} \in [0,1]^{N^x\times N^y} \end{aligned} \tag{1}$$

Here, λ_c and J represent the wavelength of interest and the injected light source, respectively. The design variables, θ, first parameterize the design patterns through $\mathcal{P}$. This is followed by a combination of projections $\mathcal{G}$ applied to the parameterized pattern ρ to generate the final device design, $\bar{\rho}$, in which various heuristics have been proposed in previous works to minimize the gap between the numerically optimized device performance and the post-fabrication performance [12]–[16]. The design patterns $\bar{\rho}$ are then passed into a numerical solver (e.g., FDFD or FDTD) to perform forward and adjoint simulations. Finally, using the calculated adjoint gradient, backpropagation updates the design variables, enabling iterative optimization of the design.

B. Machine Learning-Assisted Photonic Inverse Design

Machine learning-assisted photonic inverse design methods can generally be categorized into two classes: generative methods and predictive methods, for now `MAPS` only support predictive model while the generative models are left for future develop.

The predictive method focuses on approximating the response of given design patterns. Traditionally, these responses are computed using numerical solvers that solve Maxwell's equations in either the time domain (FDTD) or the frequency domain (FDFD). Previous works [17], [18] have treated forward simulations as a black box, directly predicting specific quantities such as S-parameters. Other studies [10], [11], [19] have attempted to predict the electric or magnetic field distributions for a given design.

Despite the progress made, most efforts in predictive ML-assisted photonic inverse design to date have primarily concentrated on model development to achieve better approximations, among which the datasets, problem formulations, and evaluation metrics vary, resulting in difficulty in direct comparison.

III. Proposed `MAPS` Infrastructure

Figure 1 illustrates the main framework of the `MAPS` infrastructure, which comprises three key components. The first is a dataset, `MAPS-Data`, featuring a balanced and more realistic data distribution. It covers a diverse range of photonic devices and includes rich labels to support universal training and evaluation of various AI-based PDE solvers. The second component is a PDE solver training framework, `MAPS-Train`, which enables the training of AI models with different formulations and provides a unified, comprehensive evaluation

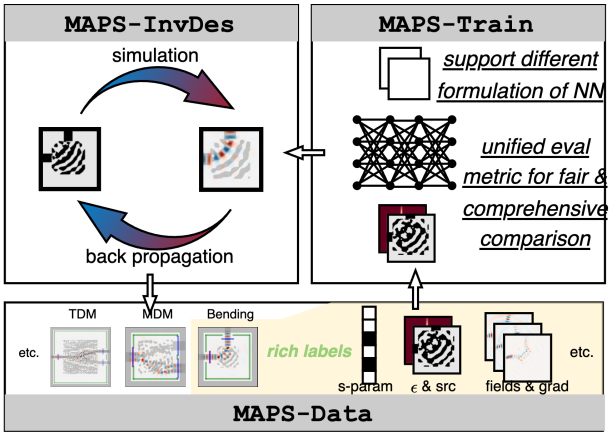

Fig. 1: Illustration of `MAPS` infrastructure.

of their performance. Finally, the inverse design framework, `MAPS-InvDes`, offers high flexibility and user-friendliness, seamlessly integrating with AI-based PDE solvers to streamline the design process.

A. `MAPS-Data`: A Dataset Balanced, More Reasonable Data Distribution and Rich Label Supporting Universal Training and Throughout Evaluation

Data is critical to AI-assisted photonic device simulation and inverse design, e.g., performance prediction, forward field simulation, and inverse structure generation. An ideal dataset for training models in photonic inverse design should possess the following properties: (1) it includes representative device structures that comprehensively cover the vast inverse design space, and (2) it should include detailed, informative labels to fully characterize the state of each sample and provide strong supervision to the model learning process. However, creating such an ideal dataset presents significant challenges. Given the high cost of data acquisition through numerical simulation and high-dimensional design space, the scarcity of large-scale, high-quality labeled data becomes a significant barrier to hindering model training and generalization. Efficient sampling strategies need to be explored to facilitate better model learning while maintaining high data acquisition efficiency; Simply increasing data volume is prohibitively costly and thus not practical in resolving the generalization dilemma for current AI models.

To address this fundamental challenge, we propose `MAPS-Data`, as shown in Fig. 2, a dataset acquisition framework that features: (1) a flexibly configurable scheme to support the exploration of diverse data collection strategies; (2) support the generation of rich, informative labels that thoroughly characterize each sample's state and figure-of-merits (FoMs) in the space that is interested specifically in inverse design's usage; (3) support of multi-fidelity simulation data generation that enables a trade-off between the data acquisition cost and dataset quality. and (4) covers a wide variety of photonic devices, ranging from simple to complex, single-function to multiplexed, and passive to active components. Next, we will elaborate on the unique features of `MAPS-Data` and delve into their significance to AI-assisted photonic device design.

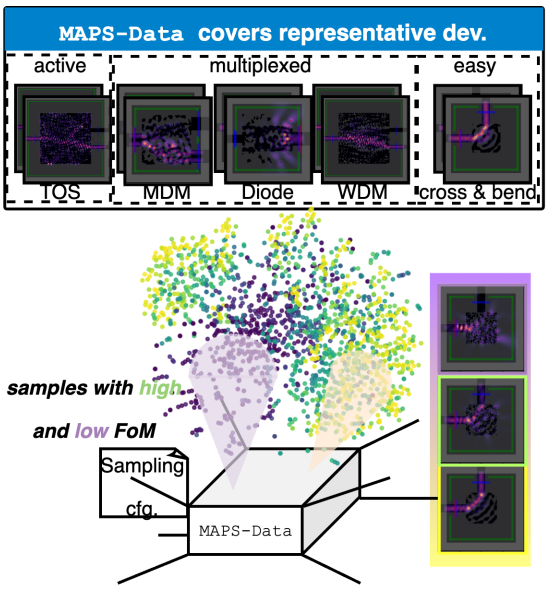

Fig. 2: MAPS-Data framework with various devices and sampling strategies.

1) Flexibly Configurable Data Sampling Strategy: Given a limited data acquisition cost budget, it is critical to intelligently sample the most representative design points for simulation and label generation. The actual device structures encountered by an adjoint gradient-based inverse device optimizer, as discussed in Section II-A, encompass soft structure patterns with low FoMs in the early stage and gradually transition to hard binarized structure with high FoMs when it converges. However, most prior work usually predefines a design space with tunable design knots and randomly sample structures from the space, This strategy only includes binarized design patterns [10], [20] with low FoMs and often fails to train a generalizable model to support inverse design.

A natural question arises: *How to strategically select data samples to approach the real distribution that the AI model encountered in the actual query during device inverse design?* To facilitate the exploration of alternative sampling strategies, MAPS-Data provides a flexibly configurable framework that allows users to easily customize sampling approaches during data acquisition. MAPS-InvDes model is seamlessly integrated with MAPS-Data to enable an optimization-aware data sampling approach. When integrated with MAPS-Train, the sampled dataset can be used to train various AI models to evaluate its effectiveness using multiple device-specific metrics, enabling fair and comprehensive comparisons between different strategies.

2) Rich Labels for Multi-task Learning and Evaluation: The rapid development of diverse machine learning methods for addressing the forward simulation and inverse design of photonic devices has introduced significant variability in their label requirements. For instance, black-box models often predict the S-parameters of specific devices, whereas models pursuing interpretability or adjoint gradients may predict electric or magnetic field distributions. To accommodate this diversity and fully leverage the information in a limited number of data samples, MAPS-Data extracts rich labels from simulation results, including transmission, reflection, radiation, electrical/magnetic fields, adjoint gradient under a certain objective, Maxwell equation matrices, etc. With rich labels for each data sample, we can support the multi-task supervised and self-supervised learning, ensuring broad applicability and flexibility.

3) Varying-Fidelity Data for Robust, Efficient Multi-Fidelity Model Training:

Multi-fidelity datasets provide device simulation results at varying quality levels, balancing the trade-off between data acquisition efficiency and quality. High-fidelity data, such as simulations of high-performance devices computed with fine mesh granularity, require significantly more computational resources, sometimes even require a time-consuming optimization process to find the structure, but offer more reliable supervision for training AI models. In contrast, low-fidelity data with random patterns simulated with coarser mesh granularity are computationally inexpensive but less accurate and informative. In numerical simulation literature, methods like Richardson extrapolation demonstrate how low-fidelity solutions can be systematically refined to approximate high-resolution results. This creates opportunities for AI models to integrate abundant low-fidelity data with a limited amount of high-fidelity data, enhancing generalization while maintaining data efficiency. By strategically leveraging these data sources, AI models can achieve robust performance with reduced data collection cost. For generative AI models used in device inverse design, training datasets primarily consist of low-performance devices. High-performance devices, being the optimization target, are generally unavailable during training. This necessitates the use of low-FoM devices in the training phase, which further underscores the importance of multi-fidelity property of MAPS-Data. To advance research in multi-fidelity modeling, MAPS-Data provides *paired device simulation data across fidelity levels*, enabling comprehensive exploration of fidelity-driven trade-offs in AI model training.

4) A Broad Design Space of Representative Device Types: As illustrated in Fig. 2, MAPS-Data encompasses a diverse range of inverse-designed photonic devices, from relatively simple structures like waveguide bends and crossings to more intricate designs, including optical diodes, wavelength division multiplexers (WDM), mode division multiplexers (MDM), and active thermo-optic switches (TOS). This extensive collection spans both single-function and multiplexing devices, as well as passive and active components, offering a comprehensive dataset with varying levels of complexity. These devices represent diverse parameter dimensions in the device structure and operation, including variations in permittivity distribution, input light source wavelength, optical mode, and incident port locations. The dataset incorporates multiple design targets and performance metrics, making it a robust benchmarking platform for multi-task learning across a spectrum of challenges. By capturing devices of varying difficulty levels, MAPS-Data supports the development of models capable of addressing complex, real-world design problems.

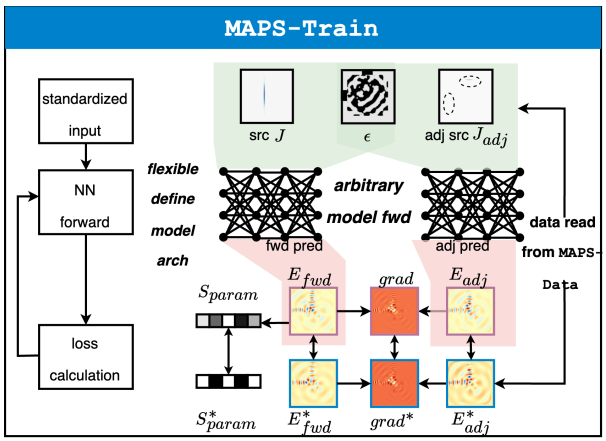

Fig. 3: MAPS-Train framework.

B. MAPS-Train: A Training Infrastructure Tailored for ML-assisted Photonic Device Inverse Design

The success of AI-assisted photonic device simulation and inverse design hinges not only on the quality of the data but also on the model architecture and training procedures. Previous work [10], [21] has shown that improved model architectures and training methods, e.g., with physics-inspired modules, data augmentation, and loss functions, can significantly enhance optical simulation performance. As AI models adopt diverse approaches to photonic device simulation and inverse design—particularly with advancements in physics-informed AI and multi-task learning—it becomes essential for training procedures to adapt accordingly. This includes supporting flexible training logic and enabling the construction of both data-driven and physics-driven loss functions. A critical component of effective training is standardized model testing, which ensures consistent evaluation and facilitates fair comparisons across methods. Standardized metrics play a pivotal role in benchmarking models reliably. To meet these needs, an ideal training framework for photonic device design must satisfy the following criteria: (1) Researchers should be able to define any model architecture conveniently, including ensembles or cascades of models, such as Tandem neural networks and generative adversarial networks (GANs). (2) The framework should support flexible training workflows tailored to specific problem formulations, such as multi-task learning, distillation, pretraining and fine-tuning, multi-stage learning, and autoression. Additionally, it must enable the incorporation of diverse loss functions, including data-driven (e.g., normalized MSE) and physics-driven (e.g., Maxwell equation residual) objectives. (3) Evaluation should adhere to standardized metrics to ensure fair and consistent benchmarking. This includes general regression metrics and domain-specific criteria, such as S-parameter prediction error and adjoint gradient alignment.

To satisfy the above demand in model training, we develop MAPS-Train, as illustrated in Fig. 3. MAPS-Train offers the following key features: (1) **Hierarchical Data Loader Pipeline**: This pipeline partition data samples at the device level to prevent test set leakage and aggregates multiple sources or ports for each device, enabling effective data augmentation (e.g., superposition-based Mixup [22]). (2) **Flexible Model Architecture Definition**: A flexible interface for defining model architectures, including different data encoding operators, model backbones, task-specific heads, and multi-model setups (e.g., Tandem neural networks) for both forward prediction and inverse generation. (3) **Customizable Training Procedures**: The framework supports a wide range of training workflows, integrating data-driven loss functions (e.g., normalized MSE) and physics-driven loss components (e.g., Maxwell equation residual). (4) **Comprehensive Model Evaluation**: Standardized evaluation metrics are included, ranging from regression errors to specialized metrics for inverse design, such as S-parameter prediction errors and adjoint gradient alignment.

1) Flexibility and Extensibility: Previous studies [10], [19], [23], have shown that physics priors and the manner in which a model is conditioned on its input can significantly impact the performance of AI solvers. MAPS-Train provides a flexible framework for modifying network architectures, enabling the incorporation of additional ansatz into model designs to develop more advanced and effective AI solvers.

2) A Unified Framework and Standardized Evaluation Metrics: Comparing AI solvers has been difficult due to variations in datasets, problem formulations, and evaluation metrics. MAPS-Data addresses dataset inconsistencies, but differences in source representation and metrics—e.g., NMSE of S-parameters vs. normalized L_2 norm—complicate fair comparisons. MAPS-Train resolves these issues by standardizing model inputs (permittivity ϵ and source J, as shown in Fig. 1 and Fig. 3) and providing a comprehensive label set. It introduces gradient similarity as a key metric, critical for ensuring accurate optimization convergence. By integrating MAPS-Data's unified datasets with MAPS-Train's standardized metrics, this framework fosters fair benchmarking and collaboration in photonics machine learning.

C. MAPS-InvDes: AI-Assisted Fabrication-Aware Adjoint Inverse Design Framework

Adjoint-based inverse design explores high-dimensional design spaces, enabling compact, high-performance photonic devices. However, its practical adoption is limited due to challenges such as: (1) Modest performance improvements in key metrics (e.g., insertion loss, bandwidth) compared to manual designs; (2) High computational demands from iterative simulations; (3) Performance degradation post-fabrication due to sensitivity to manufacturing variations; (4) Non-intuitive structures that hinder interpretability and trust.

To address these challenges, advanced techniques are required for optimization, initialization, fabrication constraints, and accessible physics abstraction.

MAPS-InvDes, illustrated in Fig. 4, provides: (1) Easy definition of complex device structures; (2) Advanced topology parametrization for shape and size optimization; (3) Built-in options for initialization, constraints, and variation modeling; (4) Predefined and customizable optimization objectives with minimal physics expertise; (5) Integration with MAPS-Train 's pre-trained AI solvers for efficient, AI-driven design.

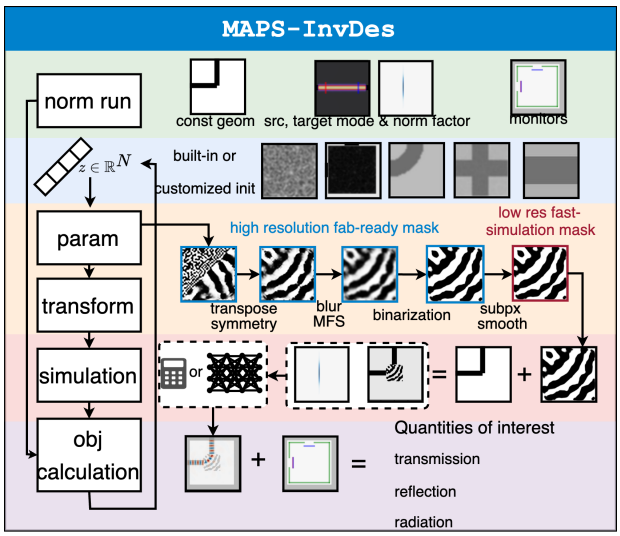

Fig. 4: `MAPS-InvDes` framework.

1) Initialization: Adjoint-based inverse design is highly sensitive to initialization due to its high-dimensional, non-convex nature [16]. To address this, `MAPS-InvDes` includes predefined schemes for smooth convergence and supports custom initialization for refining manual designs.

2) Constraints and Reparametrization: To enhance manufacturability, `MAPS-InvDes` applies constraints like symmetry and minimum feature size (MFS) through extensible, differentiable transformations. Fabrication constraints, such as lithography and etching models, are seamlessly embedded for end-to-end optimization.

3) Variation-Aware Inverse Design: Ensuring manufacturability and robustness against variations is crucial. `MAPS-InvDes` incorporates a differentiable lithography model [24] for robust optimization in manufacturable subspaces. It also supports integrating advanced AI-based fabrication models for adaptability.

4) Optimization Objectives: Photonic inverse design often requires expertise in defining objectives like far-field projection or eigenmode coefficients. `MAPS-InvDes` simplifies this with a suite of pre-defined, composable objectives, such as transmission and far-field intensity, allowing users to specify design targets with minimal knowledge.

IV. Case Studies

A. Result on the different methods to sample the data

The first case study using `MAPS` explores data sampling strategies versus random sampling. An ideal dataset must span the full design space, including low- and high-performance device patterns. Random sampling mainly yields low-performing devices, limiting the model's ability to predict high-performance patterns. Sampling along optimization trajectories captures diverse designs while avoiding redundancy in late-stage patterns.

Figure 5(a) shows random sampling of a bending waveguide produces low transmission efficiency (<10%) in most samples. Optimization trajectory-based sampling includes a broader range but results in an unbalanced distribution. Perturbations

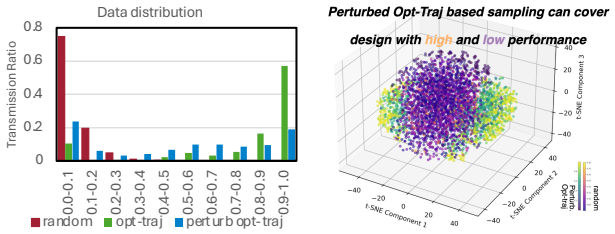

(a) (b)

Fig. 5: Comparison of sampling strategies: (a) Transmission ratio histogram for different strategies; (b) t-SNE showing separate distributions of low- and high-performance patterns, with perturbed opt-traj sampling covering both.

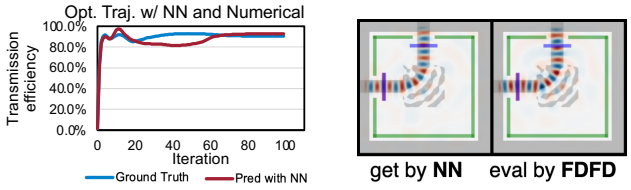

(a) (b)

Fig. 6: Gradient purely comes from NN (a) evaluation result provided by FDFD and NN (b) the field response of final design predicted by NN and verified by FDFD

during data selection address this imbalance, creating a more balanced distribution. To assess dataset strategies, we trained two baselines on different datasets and evaluated them using normalized L_2 norm and gradient similarity. Results in Table I show models trained on perturbed trajectory sampling outperform random sampling, achieving better prediction accuracy and gradient similarity.

B. Gradient Computation Methods: Adjoint Fields vs. Auto-Diff

Predictive models in inverse design face a key challenge: gradient computation. There are two main approaches: (1) Black-box models or forward field predictors rely on auto-differentiation. (2) Field predictors compute gradients directly from forward and adjoint fields. Table II highlights that using

TABLE I: Compared to randomly sampled dataset, model trained on perturbed Opt-Traj dataset can provide better gradient similarity and more accurate field prediction.

models	dataset	Train N-L2norm	Test N-L2norm	Grad Similarity
FNO	Perturb Opt-Traj	0.1018	0.1881	0.42704
	random	0.1122	0.7910	0.08313
Unet	Perturb Opt-Traj	0.4120	0.3401	0.27068
	random	0.5881	0.8290	0.02893

TABLE II: Comparison between different gradient calculation methods. The gradient calculated from the predicted forward and adjoint field is the most accurate

models	Grad Method	Grad Similarity
FNO	AD-Black Box	0.0511
	AD-Pred Field	0.0552
	Fwd & Adj Field	0.4270
Unet	AD-Black Box	0.0243
	AD-Pred Field	0.0406
	Fwd & Adj Field	0.2707

TABLE III: Comparison accross different predictive baselines on different benchmark devices, the result format is Train N-L2norm/Test N-L2norm/Test gradient similarity

Baselines	bending	crossing	optical diode
FNO	0.10/0.19/0.43	0.08/0.08/0.83	0.16/0.83/0.08
F-FNO	0.13/0.14/0.58	0.11/0.08/0.86	0.16/0.72/0.12
Unet	0.41/0.34/0.25	0.38/0.30/0.65	0.53/0.87/0.03
NeurOLight	0.11/0.14/0.55	0.10/0.08/0.84	0.14/0.71/0.14
	MDM	WDM	TOS
FNO	0.25/0.58/0.20	0.56/0.87/0.03	0.45/1.01/0.02
F-FNO	0.30/0.47/0.31	0.60/0.75/0.06	0.52/0.99/0.03
Unet	0.71/0.76/0.13	0.85/0.88/0.00	0.82/0.99/0.00
NeurOLight	0.27/0.45/0.31	0.71/0.73/0.10	0.70/0.94/0.03

forward and adjoint fields yields higher gradient accuracy compared to auto-diff.

C. Main Results

We evaluated four baseline models—FNO, Factorized-FNO, UNet, and NeurOLight—on benchmark devices (Table III). Models were trained using the normalized L_2 norm between the predicted and ground truth fields (E_z, H_x, H_y). Magnetic fields H_x and H_y were derived from the predicted E_z. NeurOLight outperformed others in field prediction and gradient alignment. However, for complex patterns, none of the models performed satisfactorily, indicating the need for more advanced approaches.

D. Integrate Neural Solver to `MAPS-InvDes`

As the last case study, we would like to show the integration of the model trained from `MAPS-Train` to replace the numerical solver. Figure 6 shows the optimization trajectory purely driven by NN and the evaluation at each iteration using FDFD as the ground truth.

V. Conclusion

In this work, we introduced `MAPS`, a multi-fidelity AI-augmented photonic simulation and inverse design infrastructure. Through various case studies, we demonstrated `MAPS`'s versatility in data acquisition, model training, and implementing an AI-assisted adjoint-based inverse design framework, showcasing its potential to advance photonic hardware design and scientific machine learning.

References

[1] E. W. Wang, D. Sell, T. Phan, and J. A. Fan, "Robust design of topology-optimized metasurfaces," *Optical Materials Express*, vol. 9, no. 2, pp. 469–482, 2019.

[2] A. M. Hammond, A. Oskooi, S. G. Johnson, and S. E. Ralph, "Photonic topology optimization with semiconductor-foundry design-rule constraints," *Optics Express*, vol. 29, no. 15, pp. 23 916–23 938, 2021.

[3] T. W. Hughes, I. A. Williamson, M. Minkov, and S. Fan, "Forward-mode differentiation of maxwell's equations," *ACS Photonics*, vol. 6, no. 11, pp. 3010–3016, 2019.

[4] F. Wang, J. S. Jensen, and O. Sigmund, "Robust topology optimization of photonic crystal waveguides with tailored dispersion properties," *JOSA B*, vol. 28, no. 3, pp. 387–397, 2011.

[5] M. Schevenels, B. Lazarov, and O. Sigmund, "Robust topology optimization accounting for spatially varying manufacturing errors," *Computer Methods in Applied Mechanics and Engineering*, vol. 200, no. 49, pp. 3613–3627, 2011. [Online]. Available: https://www.sciencedirect.com/science/article/pii/S0045782511002611

[6] Z. Li, N. Kovachki, K. Azizzadenesheli, B. Liu, K. Bhattacharya, A. Stuart, and A. Anandkumar, "Fourier neural operator for parametric partial differential equations," 2021. [Online]. Available: https://arxiv.org/abs/2010.08895

[7] A. Tran, A. Mathews, L. Xie, and C. S. Ong, "Factorized fourier neural operators," 2023. [Online]. Available: https://arxiv.org/abs/2111.13802

[8] O. Ronneberger, P. Fischer, and T. Brox, "U-net: Convolutional networks for biomedical image segmentation," 2015. [Online]. Available: https://arxiv.org/abs/1505.04597

[9] X. Zhang, J. Helwig, Y. Lin, Y. Xie, C. Fu, S. Wojtowytsch, and S. Ji, "Sinenet: Learning temporal dynamics in time-dependent partial differential equations," in *The Twelfth International Conference on Learning Representations*, 2024. [Online]. Available: https://openreview.net/forum?id=LSYhE2hLWG

[10] J. Gu, Z. Gao, C. Feng, H. Zhu, R. T. Chen, D. S. Boning, and D. Z. Pan, "Neurolight: A physics-agnostic neural operator enabling parametric photonic device simulation," in *Conference on Neural Information Processing Systems (NeurIPS)*, 2022.

[11] G. C. S. N. R. C. J. G. Hanqing Zhu, Wenyan Cong and D. Z. Pan, "Pace: Pacing operator learning to accurate optical field simulation for complicated photonic devices," in *Conference on Neural Information Processing Systems (NeurIPS)*, 2024.

[12] E. Khoram, X. Qian, M. Yuan, and Z. Yu, "Controlling the minimal feature sizes in adjoint optimization of nanophotonic devices using b-spline surfaces," *Optics Express*, vol. 28, no. 5, pp. 7060–7069, 2020.

[13] M. F. Schubert, A. K. Cheung, I. A. Williamson, A. Spyra, and D. H. Alexander, "Inverse design of photonic devices with strict foundry fabrication constraints," *ACS Photonics*, vol. 9, no. 7, pp. 2327–2336, 2022.

[14] M. Chen, J. Jiang, and J. A. Fan, "Design space reparameterization enforces hard geometric constraints in inverse-designed nanophotonic devices," *ACS Photonics*, vol. 7, no. 11, pp. 3141–3151, 2020. [Online]. Available: https://doi.org/10.1021/acsphotonics.0c01202

[15] E. Gershnabel, M. Chen, C. Mao, E. W. Wang, P. Lalanne, and J. A. Fan, "Reparameterization approach to gradient-based inverse design of three-dimensional nanophotonic devices," *ACS Photonics*, vol. 10, no. 4, pp. 815–823, 2022.

[16] P. Ma, Z. Gao, A. Begovic, M. Zhang, H. Yang, H. Ren, Z. R. Huang, D. Boning, and J. Gu, "Boson^{-1}: Understanding and enabling physically-robust photonic inverse design with adaptive variation-aware subspace optimization," 2024. [Online]. Available: https://arxiv.org/abs/2411.08210

[17] R. Zhu, T. Qiu, J. Wang, S. Sui, C. Hao, T. Liu, Y. Li, M. Feng, A. Zhang, C.-W. Qiu *et al.*, "Phase-to-pattern inverse design paradigm for fast realization of functional metasurfaces via transfer learning," *Nature communications*, vol. 12, no. 1, p. 2974, 2021.

[18] H. Lin, J. Hou, J. jin, Y. Wang, R. Tang, X. Shi, Y. Tian, and W. Xu, "Machine-learning-assisted inverse design of scattering enhanced metasurface," *Opt. Express*, vol. 30, no. 2, pp. 3076–3088, Jan 2022. [Online]. Available: https://opg.optica.org/oe/abstract.cfm?URI=oe-30-2-3076

[19] P. Ma, H. Yang, Z. Gao, D. S. Boning, and J. Gu, "Pic2o-sim: A physics-inspired causality-aware dynamic convolutional neural operator for ultra-fast photonic device fdtd simulation," 2024. [Online]. Available: https://arxiv.org/abs/2406.17810

[20] P. Naseri and S. V. Hum, "A generative machine learning-based approach for inverse design of multilayer metasurfaces," *IEEE Transactions on Antennas and Propagation*, vol. 69, no. 9, pp. 5725–5739, 2021.

[21] Z. Li, H. Zheng, N. Kovachki, D. Jin, H. Chen, B. Liu, K. Azizzadenesheli, and A. Anandkumar, "Physics-informed neural operator for learning partial differential equations," 2023. [Online]. Available: https://arxiv.org/abs/2111.03794

[22] J. Gu, Z. Gao, C. Feng, H. Zhu, R. T. Chen, D. S. Boning, and D. Z. Pan, "NeurOLight: A Physics-Agnostic Neural Operator Enabling Parametric Photonic Device Simulation," in *Conference on Neural Information Processing Systems (NeurIPS)*, 2022.

[23] T. W. Hughes, I. A. Williamson, M. Minkov, and S. Fan, "Wave physics as an analog recurrent neural network," *Science advances*, vol. 5, no. 12, p. eaay6946, 2019.

[24] H. Yang and H. Ren, "Gpu-accelerated inverse lithography towards high quality curvy mask generation," *arXiv preprint arXiv:2411.07311*, 2024.